Desalination and Water Treatment
www.deswater.com

doi: 10.5004/dwt.2017.21715

96 (2017) 33–44
November

Increasing operational efficiency of a membrane water treatment plant using an asset management method

Chul-sung Lee, Young-wook Nam, Ji-hoon Choi, Doo-il Kim*

Department of Civil and Environmental Engineering, Dankook University, 16890, Yongin-si, Gyeonggi-do 448-701, Korea, Tel. +82-31-8005-3483; Fax: +82-31-8021-7213; emails: dikim21@dankook.ac.kr (D.-i. Kim), hiznow@hanmail.net (C.-s. Lee), youngwnam@naver.com (Y.-w. Nam), envhoon@naver.com (J.-h. Choi)

Received 31 January 2017; Accepted 21 November 2017

ABSTRACT

The life span of the pressurized hollow fiber membrane (PHFM) modules was analyzed for a full scale water treatment plant in South Korea by developing a novel mathematical model of an asset management method. The model described shifting trend and pattern of transmembrane pressure (TMP) through discrete Fourier analysis. PHFM modules suffered from problems related to weakened material properties and reduced life span because of frequent cleaning in place. Thus, the plant will need to replace deteriorated PHFMs with new ones at uncertain time slot in the future. The replacement time slot anticipated in this study as first, was March 2018 for technical efficiency and September 2015 for economic efficiency when the benefit coefficient, related to raw water quantity, was 0.100. However, this study indicated that the result of economic efficiency could be improved by March 2018 when its benefit coefficient was increased to be 0.127 for about 3 years. Therefore, this system will extend longevity without financial burdens through the minimum raise of its benefit coefficient. The plant could take time to prepare a replacement of PHFM and to find ways to lessen the burden of operation and maintenance in a few years. It also showed that the trend of TMP would steadily increase in a few years, which implies that various technical problems would frequently occur in the system.

Keywords: Membrane; Water treatment; Transmembrane pressure (TMP); Asset management; Discrete Fourier frequency analysis; Benefit–cost analysis

1. Introduction

Asset management (AM) is operation and maintenance (O&M) method to maintain the value of assets in the long-term, based on the triple-bottom-line thinking that integrates social, environment, and economic responsibilities [1,2]. AM focuses on a key role component of the utility, which is considered as a main asset [3]. AM is used foraging infrastructures such as bridges, roads, water distribution systems, and water treatment utilities [4]. The sum of O&M cost in aging infrastructures is not small when compared with their construction cost in the long-term because the O&M cost tends to increase gradually when structures are aged [5,6]. Thus, the O&M cost increases the burden of financial circumstances in the long-term which requires reducing O&M cost in aging infrastructures using AM methods [7,8].

However, the research of using an AM method in water treatment utilities is marginal. This study applied the AM method to a water treatment utility in the Republic of Korea which is using pressurized hollow fiber membrane (PHFM) modules. The water treatment plant has been enterprising from July 2011 to present, showing that its PHFM modules are currently aging and its O&M costs are gradually increasing in these days. The O&M cost of the membrane-purifying plant is larger than conventional treatment plants [9–11]. The cost is also influenced by the aging degree of PHFM modules [12]. The aging of the modules implies the

* Corresponding author.

Presented at the 9th International Conference on Challenges in Environmental Science & Engineering (CESE-2016), 6–10 November 2016, Kaohsiung, Taiwan.

increased frequency of the cleaning in place (CIP) [13,14] and the increased transmembrane pressure (TMP) [15,16]. Thus, the aging modules need to be replaced with new ones at the proper time to improve the O&M efficiency and to reduce O&M cost in a plant. There are existing methods to alert the replacement time of the PHFM modules. They are monitoring the flow of the membrane filters [17], testing the air bubble through the membrane modules [18–20], and measuring the change of TMP [21,22]. These technical skills are dependent on the practical experience of administrators in water treatment utilities as well as limited possibilities the exact renewal time to be in a short-term scale. To overcome these limits of existing skills, administrators of plants needs to use an AM method which could anticipate the time of replacement of the main asset in the plant in long-term scale [23] as well as to help enterprising efficiently the O&M of plants in the economic view [24], which makes an AM become more important in the management of aged utilities [8].

The objective of this paper is (1) to develop a mathematical model for AM analysis of the PHFM modules, (2) to verify the model using the full scale field data, (3) to estimate the replacing time slot of the PHFM modules, and (4) to find alternatives reducing the load of O&M part for sustainable management in the plant.

2. Model development

2.1. Developing mathematical TMP model to find the technical life span

The relation between the permeate flux penetrating pores of membranes (L/m^2/h), Ψ_{pore}, and TMP is defined in Eq. (1) without the osmotic effect generated by the difference of solute density between feed water and purified water, according to Hagen–Poiseuille formula [25–27].

$$\text{TMP} = \frac{32 \cdot \delta_m \cdot \mu_s}{\varepsilon_m \cdot D_p^2} \cdot \Psi_{\text{pore}}, k_w = \frac{\varepsilon_m \cdot D_p^2}{32 \cdot \delta_m \cdot \mu_s} \tag{1}$$

Here, the mass-transfer coefficient (k_w) includes fluidic characteristics such as viscosity (μ_s) and membrane characteristics such as pore porosity (ε_m), pore diameter (D_p), membrane's thickness (δ_m) as shown in Fig. 1.

A sieve effect is dominant to screen particles for UF membrane and MF membrane when the water flows through membrane's pores in which the diameter influences on the magnitude of flux [28]. Particles in the fluid stack over the pores' surface, which decrease the magnitude of flux [29,30]. As a result, the magnitude of TMP tends to increase in order to keep constant flux [31,32]. Thus, the dominant factor can be the particle's density in feed water in the sieve effect as shown in Fig. 1(b).

When particles adhere to the surface on the pore wall of membrane, these particles could make the membrane deteriorated, which influences the decrease of CIP efficiency [33,34]. Although these accumulated particles can mostly be washed out by cleaning chemicals like NaOCl, H_2SO_4, and other stronger oxidants in CIP process, it is not completely recovered into the virgin state of membrane [35]. Since H_2SO_4 or another stronger oxidants influence physical characteristics, repeated CIP makes physical characteristics of membrane gradually weaker [36,37]. This can become more critical in higher TMP circumstances [38–40]. Thus, the deterioration degree of membrane becomes worse by increasing the operating time (Δt) and the number of CIP, which is defined as the number of operation (N). These happenings can be formulated as Eq. (2), which describes the TMP increase using the operating time (Δt) and the number of operation (N).

$$\Delta\text{TMP}(t, N) = \Delta t \cdot \frac{\partial \text{TMP}}{\partial t} + \Delta N \cdot \frac{\partial \text{TMP}}{\partial N} \tag{2}$$

where ∂TMP/∂t is the slope of TMP over the operating time (Δt), and ∂TMP/∂N is the slope of TMP over the number of operation (N). They are defined in Eqs. (3) and (4), respectively, from Eqs. (1) and (2).

$$\frac{\partial \text{TMP}}{\partial t} = \frac{32 \cdot \delta_m \cdot \mu_s}{\varepsilon_m} \cdot \frac{\partial}{\partial}\left(\frac{1}{D_p^2}\right) \tag{3}$$

$$\frac{\partial \text{TMP}}{\partial N} = \frac{32 \cdot \delta_m \cdot \mu_s}{\varepsilon_m} \cdot \frac{\partial}{\partial N}\left(\frac{\Psi_{\text{pore}}}{D_p^2}\right) \tag{4}$$

As shown in Eq. (3), ∂TMP/∂t has membrane's properties and depends on the pore diameter. When ∂TMP/∂t is constant in an assumption that the pore diameter is not drastically changed in each Nth, TMP shows the linear increase over the operational time with the slope for each Nth. And ∂TMP/∂N also has membrane's properties and dependence on both the pore diameter and flux as shown in Eq. (4).

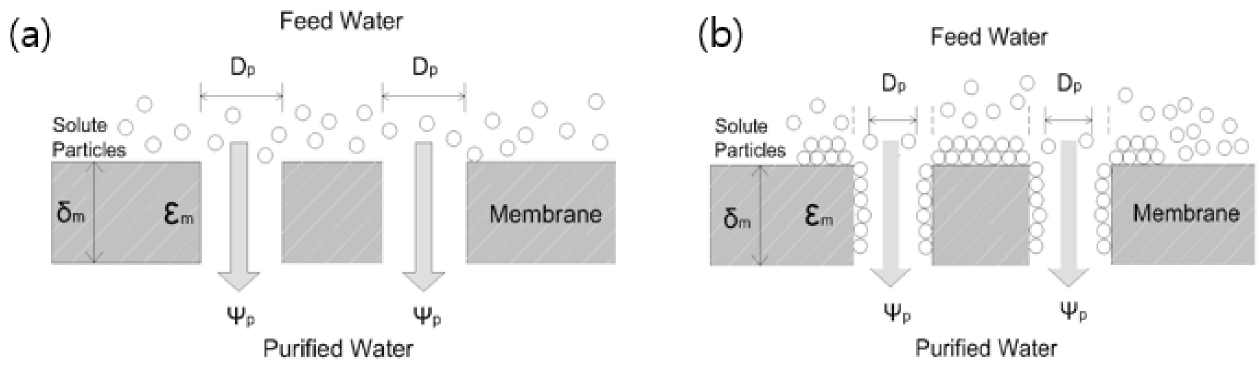

Fig. 1. Particles sticking to membrane surface and pores: (a) virgin state and (b) partly fouled state.

Because ∂TMP/∂N is related to the membrane deterioration factor (α_d), the frequency factor of particles' density and flux, the slope $\alpha(N)$ on Nth can be shown in Eq. (5) using the linear combination method [41].

$$\alpha(N) = \frac{\Delta\text{TMP}(t,N)}{\Delta t(N)} = \alpha_d \cdot N + Z_{\text{NTU\&Flux}}(N) \quad (5)$$

Here, the membrane deterioration factor (α_d) trend to increase with $\alpha(N)$ values on Nth. And, $Z_{\text{NTU\&Flux}}(N)$ is the trend function of $\alpha(N)$ having the same frequencies of NTU(N) and Flux(N) on N domain. The particles' density is indirectly measured by Nephelometric Turbidity Unit (NTU).

Based on the assumption of the linear increase of TMP in Nth stage, TMP could be modelled as Fig. 2. TMP will increase from TMP_b to TMP_h with the slope $\alpha(N)$ for the operational time (Δt) within each Nth stage, which can be formulated as Eq. (6).

$$\text{TMP}_h(N) = \text{TMP}_b(N) + \Delta t(N)\cdot\alpha(N) \quad (6)$$

The difference (ΔTMP) between TMP_b and TMP_h in Nth stage is also shown in Eq. (7). Where TMP_b is the bottom value of Nth stage, and TMP_h is the highest value of Nth stage.

$$\Delta\text{TMP}(N) = \text{TMP}_h(N) - \text{TMP}_b(N) \quad (7)$$

When $\Delta t(N)$ is defined as the operational time in Nth stage, the operational time in (N + 1)th stage, $\Delta t(N + 1)$, is defined in Eq. (8) with $\Gamma(N)$ that is the ratio of the operational time from N to $N + 1$.

$$\Delta t(N+1) = \Delta t(N)\cdot\Gamma(N+1) \quad (8)$$

Thus, TMP_b in $N + 1$ stage is defined in Eq. (9) with $R(N)$ of N stage, which describes the TMP decrease after Nth CIP. Where $R(N)$ is the recovery ratio, which is generally over 95% when TMP is recovered by washing particles adhered to the fouled membrane surface during CIP. However, $R(N)$ could be influenced by the deteriorating degree of the active membrane [42], which was theoretically decreased through increasing the number of CIP [43].

$$\text{TMP}_b(N+1) = \text{TMP}_h(N) - \Delta\text{TMP}(N)\cdot R(N) \quad (9)$$

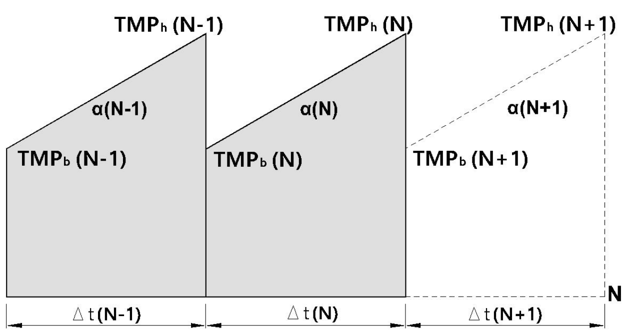

Fig. 2. The effect of repeated chemical cleanings on TMP.

The area of TMP on Nth is evaluated by using Eq. (10), which could be used to estimate the operational cost because TMP is generated by a pressurizing pump in the plant which consumes electricity.

$$\text{Area}_{\text{TMP}}(N) = \frac{\text{TMP}_h(N) + \text{TMP}_b(N)}{2}\cdot\Delta t(N) \quad (10)$$

In order to determine the technical life span by evaluating the efficiency of active membrane based on the recovery ratio, the regeneration ratio, $E(N)$, is evaluated as Eq. (11). $E(N)$ is normally positive and possibly have values over one when many adhered particles on the membrane surface for long time are washed out during CIP.

$$E(N) = \frac{\Delta\text{TMP}(N)\cdot R(N)}{\text{TMP}_h(N) - \text{TMP}(1)} \le 0.70 \quad (11)$$

When $E(N)$ is below 0.7, the efficiency of active membrane can be finished at the N_Tth stage, which means that the membrane modules reach their life span and need to be replaced with new modules. Where 0.7 in $E(N)$ is the practical criteria that administrators in a water treatment plant use in their O&M. Therefore, the life span of membrane modules (T_{LifeSpan}) in day at N_Tth stage is calculated in Eq. (12).

$$T_{\text{LifeSpan}}(\text{day}) = \sum_{N=1}^{N_T}\left[\Delta t(N_T) + \Delta t_{\text{INS}}\right] \quad (12)$$

where Δt_{INS} is the inspection time including CIP time, which is approximately constant.

3. Materials and method

3.1. Information of full scale water treatment plant, and properties of PHFM

The full scale water treatment plant has been using the PHFM modules in its systems from July 2011 to present as shown in Fig. 3(a). The number of modules in one system is 42, having two trains in the system. The modules in the plant have not yet been renewed. The operating conditions in the plant have been ordinary in feed water qualities when comparing with other water treatment utilities in Gyeonggi and Seoul regions in South Korea. The operational data in the plant from July 2011 to September 2014 have been used in AM analysis, including TMP, O&M costs, and feed water's quality data.

The properties of the PHFM used in the water treatment plant are made from polyvinylidene fluoride as shown in Table 1. Its pore size of membrane is 0.05 μm. Inner diameter of the fiber is 0.07 mm. Outer diameter of the fiber is 1.3 mm with asymmetrical structure as shown in Figs. 3(b) and (c). Its average operating capacity per module is 112 m^3/d. Filtering velocity is 1.5 m/d. Each module is consisted of 8,900 membrane fibers. The valid surface area of its membrane is 75 m^2/module.

3.2. Using discrete Fourier analysis to find Γ(N), R(N), and α(N)

Enough O&M history data are critical in an AM analysis in order to anticipate the life span and replacing spot of

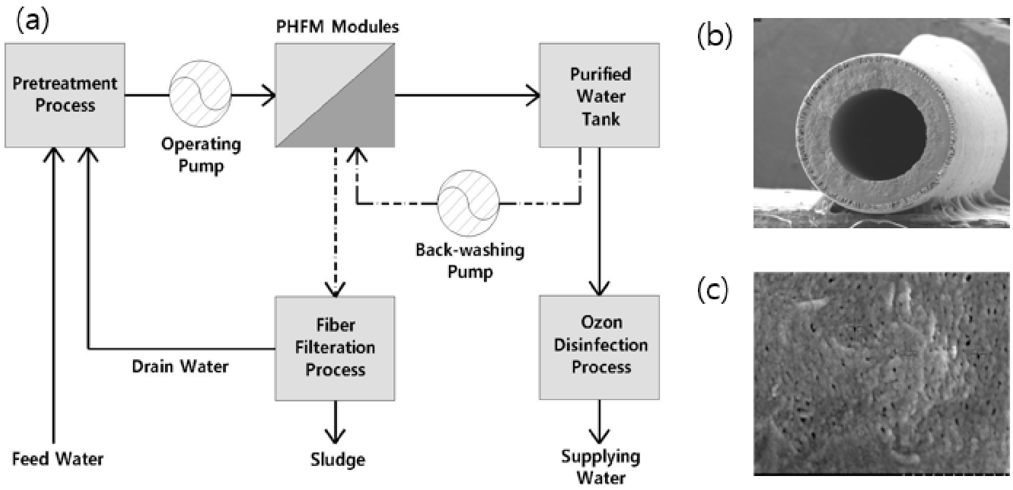

Fig. 3. The membrane system of the plant. (a) Schematic diagram of pressurized PHFM system of the water treatment plant. (b) Photo of cross-section of PHFM. (c) Photo of PHFMs surface.

Table 1
Properties of the PHFM modules

Membrane specification	
Module type	MF/UF (pressurized)
Material	Polyvinylidene fluoride (PVDF)
Bore/full Diameter	0.7/1.3 mm (asymmetric) in diameter
Capacity	112 m^3/d/module (average flow rate 1.5 m/d)
Pore size	0.05 μm
Piece of module	8,900 piece/module
Valid surface Area	75 m^2/module
Module size	216 mm × 2,300 mm

PHFM modules in the water treatment plant [44]. The O&M history data in the plant have resulted from the combined influences of the operating environment such as temperature and the fluctuation of feed water quality [45], as well as the operating know-how of administrators such as the operating pressure, the operating time, the flux, the frequency of CIP, the scale of CIP, and the others [46]. Thus, it could be assumed that the O&M history data in the plant might show periodic patterns in the long-term.

Individual inner functions such as $\Gamma(N)$, $R(N)$, and $\alpha(N)$ could be found by the summation of periodic functions because its O&M circumstances have had periodic influences in the long-term, showing characteristic patterns in $\Gamma(N)$, $R(N)$, and $\alpha(N)$. These circumstances in the long-term such as about 4 years will not massively change without higher fluctuations in the O&M conditions. These periodic patterns in the long period could be found by Fourier transformation [47], transforming from time domain signals to frequency domain ones. Fourier transformation shows its spectrums, and then its dominant frequency values could be extracted because these values could represent longer period pattern [48]. Thus, its dominant patterns in $\Gamma(N)$, $R(N)$, and $\alpha(N)$ in quasi-time domain (N) could be rebuilt by inverse transformation from frequency domain to N domain with less noises. In this study, the N domain means the number of CIP operation in a water treatment plant. Because given data types were the groups of discrete data that are not polynomial mathematical functions, Fourier series formula in discrete Fourier analysis (DFA) [49] was used in Eq. (13).

$$f(N) = \frac{a_0}{2} + \sum_{k=1}^{\infty}\left[a_k \cdot \cos\left(\frac{\pi k}{T}N\right) + b_k \cdot \sin\left(\frac{\pi k}{T}N\right)\right] \tag{13}$$

where T is the period of sample data on N domain, which could be assumed to be a half of the total period, all a_k are magnitude of cosine terms in Eq. (14), and all b_k are ones of sine terms in Eq. (15), and all d_k are ones of complex terms combined cosine terms with sine terms in Eq. (16), showing what frequencies could become dominant in periodic patterns by comparing relatively individual ones on the frequency (k).

$$a_k = \frac{a_0}{2} + \frac{2}{T}\int_0^T\left[f(N) \cdot \cos\left(\frac{\pi k}{T}N\right)\right]\mathrm{d}N, a_0 = \frac{1}{T}\int_0^T\left[f(N) \cdot 1\right]\mathrm{d}N \tag{14}$$

$$b_k = \frac{2}{T}\int_0^T\left[f(N) \cdot \sin\left(\frac{\pi k}{T}N\right)\right]\mathrm{d}N \tag{15}$$

$$d_k = \sqrt{a_k^2 + b_k^2}, \ \left(k = 0, 1, 2, 3, \ldots\right) \tag{16}$$

Furthermore, these periodic functions have individual phase differences as in Eq. (17), where M_s is the number of sampling used in the rebuilding process [50].

$$\Delta\Phi = \frac{2\pi}{M_s} \tag{17}$$

In the rebuilding process, it is important to make 'window function' in DFA to reduce errors in frequencies happened by differences between starting and ending points [51], which could make frequency's magnitudes become clearer by removing many noise frequencies in spectrum analysis.

3.3. Using B/C analysis to find the economic life span

The concept of benefit–cost (B/C) analysis has been used to assess the economic efficiency of O&M, because the *B*/*C* analysis could show the best O&M strategies from several alternatives as well as the one's economic feasibility for sustainable O&M in an AM [52]. In order to carry out *B*/*C* analysis for the plant, total O&M cost should include both its direct and indirect cost [53]. The direct cost is calculated by the summation of all O&M costs related with producing activities such as feed water cost, chemical cost for CIP, electrical cost for producing, and payroll cost for administrators. The indirect cost is evaluated by summing the lost cost influenced by temporary operational interruption and PHFM module cost spent for modules' physical failure, which are 'Values at Risk (VAR)'. VAR is evaluated by multiplying the failure probability of PHFM modules by its consequences [54–56]. The indirect cost on *N*th stage is defined in Eq. (18), and then the total O&M cost on *N*th, $C_{\text{TotalO\&M}}(N)$, becomes Eq. (19).

$$C_{\text{Indirect}}(N) = C_{\text{Loss}}(N) + C_{\text{ReplacedModule}}(N) \tag{18}$$

$$C_{\text{TotalO\&M}}(N) = C_{\text{Direct}}(N) + C_{\text{Indirect}}(N) \tag{19}$$

Benefit–cost should include only direct benefits because there is not enough quantitative information on indirect benefits [57]. Thus, benefit–cost on *N*th, $B_{\text{Produce}}(N)$, could be evaluated in Eq. (20).

$$B_{\text{Produce}}(N) = J_{\text{Water}} \cdot Q(N) \cdot \Delta t(N) \tag{20}$$

where J_{Water} is the benefit coefficient (price/ton), $Q(N)$ is the producing water quantity on *N*th, and $\Delta t(N)$ is the operating time on *N*th. The benefit–cost analysis on *N*th, $B/C(N)$ is defined in Eq. (21), which is its economic efficiency on *N*th in the O&M view [58].

$$\text{B/C}(N) = \frac{\text{B}_{\text{Produce}}(N)}{\text{C}_{\text{TotalO\&M}}(N)} \tag{21}$$

It not only shows the economic efficiency, but also indicates the happening of financial loss when $B/C(N)$ is less than one. If this situation is continued under *B*/*C* analysis, the plant will lose its economic feasibility [59], and be required to improve *B*/*C* value over one through the increase of benefit–cost or the decrease of O&M cost [60]. Thus, *B*/*C* analysis could become the crucial factor determining plant's life span and replacement time slot.

4. Results and discussion

4.1. TMP data and results of transformation from time domain to N domain

The raw data of TMP for about 1,500 d from July 2011 to September 2014 in the water treatment plant were edited into *N* domain day using the linear regression analysis [61,62]. Table 2 shows the transformation results on *N* domain. Initially, the performances of TMP appeared unstable when *N* was 1, because its TMP slope was a negative value such as –0.7556, which was not theoretically acceptable in consideration of membranes' deterioration. In addition, when *N* was 7 or 8, the system showed unstable with negative values in its TMP slope. Although some data groups, which did not follow the theoretical performance, had low values in r^2 (r^2, coefficient of determination related with the degree of linear correlation [63]), other groups had proper values in the consideration of the field circumstance.

The transformed results of TMP data on *N* domain were shown in Fig. 4 on day domain with its raw data. It appeared that the TMPs data trend could be approximately transformed into linear line even though some intervals were not proper as linear line.

4.2. Rebuilding Γ(N), R(N), and α(N) through the DFA

Some data in (N, $\Gamma(N)$) such as (2, 4.7143), (7, 3.8529), and (13, 2.5500) seems not to be proper values in the data analysis for membrane's operating time ratio because other $\Gamma(N)$ values ranged from 0.3 to 1.6. Except for these improper values, the average of the others was 0.8931 and its standard deviation was 0.4586, which showed that $\Gamma(N)$ ranged from 0.4345 to 1.3516 with its confidence level, 68% [64]. It could be assumed that $\Gamma(N)$ was approximately positioned the interval between 0.5 and 1.5 with its confidence level, 70%. Based on the interval, given $\Gamma(N)$ data were edited into 0.5 or 1.5 when $\Gamma(N)$ was below 0.5 or over 1.5, respectively.

These edited pieces of $\Gamma(N)$ data were put into the DFA, which showed magnitudes of frequency as in Figs. 5(a) and (b). When its frequency 'k' in 'a_k' was (4, 5, 8, and 11), and (4, 5, 8, 9, and 12) in 'b_k', its magnitudes of frequencies in $\Gamma(N)$ were much bigger than the other cases, which showed its valid trend. By these valid frequency values, $\Gamma(N)$ was rebuilt like in Fig. 6(c), which described its origin trend as well.

Rebuilt $\Gamma_r(N)$'s mathematical formula is shown in Eq. (22). Meanwhile, it was supposed that rebuilt $\Gamma_r(0)$was defined as 1, theoretically in the operational view. Thus, Eq. (22) would become valid when N was more than 2.

$$\begin{aligned}\Gamma_r(N) = {} & 1.0740 + 0.1376\cdot\cos\left(\frac{4\pi}{12}N - \frac{2\pi}{12}\right) \\ & + 0.1342\cdot\cos\left(\frac{5\pi}{12}N - \frac{2\pi}{12}\right) - 0.3288\cdot\cos\left(\frac{8\pi}{12}N - \frac{2\pi}{12}\right) \\ & + 0.1520\cdot\cos\left(\frac{11\pi}{12}N - \frac{2\pi}{12}\right) + 0.1867\cdot\sin\left(\frac{4\pi}{12}N - \frac{2\pi}{12}\right) \\ & + 0.1429\cdot\sin\left(\frac{5\pi}{12}N - \frac{2\pi}{12}\right) + 0.1863\cdot\sin\left(\frac{8\pi}{12}N - \frac{2\pi}{12}\right) \\ & - 0.3885\cdot\sin\left(\frac{9\pi}{12}N - \frac{2\pi}{12}\right) + 0.2638\cdot\sin\left(\frac{12\pi}{12}N - \frac{2\pi}{12}\right)\end{aligned} \tag{22}$$

Some data in (N, $R(N)$) such as (1, 0.3887), (5, –0.6320), and (8, –2.7575) seems like it is not the proper values in the data analysis for membrane's recovering ratio, because other most $R(N)$ values ranged from 0.4 to 1.6 as well as $R(N)$ was positive in the theoretical view. Except for these improper values, the average of the others was 1.0035 and its standard deviation was 0.3294, which showed that $R(N)$ ranged from

Table 2
TMP, Γ(*N*), *R*(*N*), and α(*N*) values

N	Time (d)	TMP (kPa)	Δ*t* (N)	ΔTMP	α(*N*)	r^2	Γ(*N*)	*R*(*N*)	*E*(*N*)	*Q*(*N*)
1	0.0	42.00	28.0	–22.0	–0.7966	0.9019	1.0000	0.3887	1.00	3470
	28.0	20.00								
2	28.1	29.00	132.0	11.0	0.0680	0.1466	4.7143	1.4293	1.75	4,070
	160.1	40.00								
3	160.1	24.00	159.0	49.0	0.3151	0.5695	1.2045	0.9119	1.06	3,584
	319.1	73.00								
4	319.2	28.00	75.0	30.0	0.4032	0.9702	0.4717	0.8410	0.93	3,847
	394.2	58.00								
5	394.2	33.00	110.0	11.0	0.1003	0.1332	1.4667	–0.6320	–0.53	3,869
	504.2	44.00								
6	504.3	51.00	34.0	22.0	0.6370	0.3995	0.3091	1.5887	0.83	3,348
	538.3	73.00								
7	538.3	38.00	131.0	–2.00	–0.0140	0.0046	3.8529	2.3553	–0.94	3,593
	669.3	36.00								
8	669.4	40.00	186.0	–5.00	–0.0256	0.0477	1.4198	–2.7575	3.45	3,826
	855.4	35.00								
9	855.4	22.00	96.0	30.0	0.3155	0.8075	0.5613	0.8645	1.23	4,210
	951.4	52.00								
10	951.5	26.00	75.0	21.0	0.2779	0.4874	0.7813	0.9546	1.25	4,380
	1,026.5	47.00								
11	1,026.5	27.00	123.0	24.0	0.1963	0.8130	1.6400	0.4683	0.56	4,328
	1,149.5	51.00								
12	1,149.6	40.00	60.0	8.0	0.1488	0.0486	0.487805	2.0595	0.97	4,319
	1,209.6	48.00								
13	1,209.6	31.00	153.0	10.0	0.0659	0.1950	2.55	0.9700	0.97	3,962
	1,362.6	41.00								
14	1,362.7	31.30	109.7	11.8	0.1080	0.1574	0.7171	0.9107	0.89	3,908
	1,472.4	43.15								

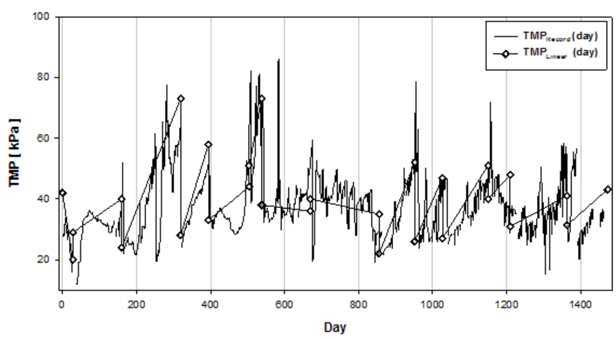

Fig. 4. TMP variation over time during the water treatment.

0.6741 to 1.3329 with its confidence level, 68%. It could be assumed that *R*(*N*) was approximately positioned the interval between 0.6 and 1.3 with its confidence level, 70%. Based on the interval, given *R*(*N*) data were edited into 0.6 or 1.3 when *R*(*N*) was below 0.6 or over 1.3, respectively.

These edited pieces of *R*(*N*) data were put into the DFA, which showed magnitudes of frequency as in Figs. 6(a) and (b). When its frequency '*k*' in 'a_k' was 4, 6, 7, 9, and 10, and its frequency '*k*' in 'b_k' was 5, 6, 8, 9, and 10, its magnitudes of frequencies in *R*(*N*) were much larger than the other cases, which showed its valid trend. By these valid frequency values, *R*(*N*) was rebuilt in Fig. 7(c), which described its origin trend as well.

Rebuilt $R_r(N)$'s mathematical formula is shown in Eq. (23). Meanwhile, it was supposed that rebuilt $R_r(0)$ and $R_r(1)$ were defined as one, because membranes theoretically were under virgin state in the membrane's physical view. Thus, Eq. (23) would become valid when *N* was more than 2.

$$\begin{aligned} R_r(N) = {} & 0.9648 + 0.1582\cdot\cos\left(\frac{4\pi}{13}N - \frac{2\pi}{13}\right) \\ & + 0.1110\cdot\cos\left(\frac{6\pi}{13}N - \frac{2\pi}{13}\right) - 0.1374\cdot\cos\left(\frac{7\pi}{13}N - \frac{2\pi}{13}\right) \\ & + 0.1256\cdot\cos\left(\frac{9\pi}{13}N - \frac{2\pi}{13}\right) - 0.1428\cdot\cos\left(\frac{10\pi}{13}N - \frac{2\pi}{13}\right) \\ & + 0.2066\cdot\sin\left(\frac{5\pi}{13}N - \frac{2\pi}{13}\right) + 0.0834\cdot\sin\left(\frac{6\pi}{13}N - \frac{2\pi}{13}\right) \\ & - 0.1562\cdot\sin\left(\frac{8\pi}{13}N - \frac{2\pi}{13}\right) - 0.0850\cdot\sin\left(\frac{9\pi}{13}N - \frac{2\pi}{13}\right) \\ & + 0.2638\cdot\sin\left(\frac{9\pi}{13}N - \frac{2\pi}{13}\right) \end{aligned} \quad (23)$$

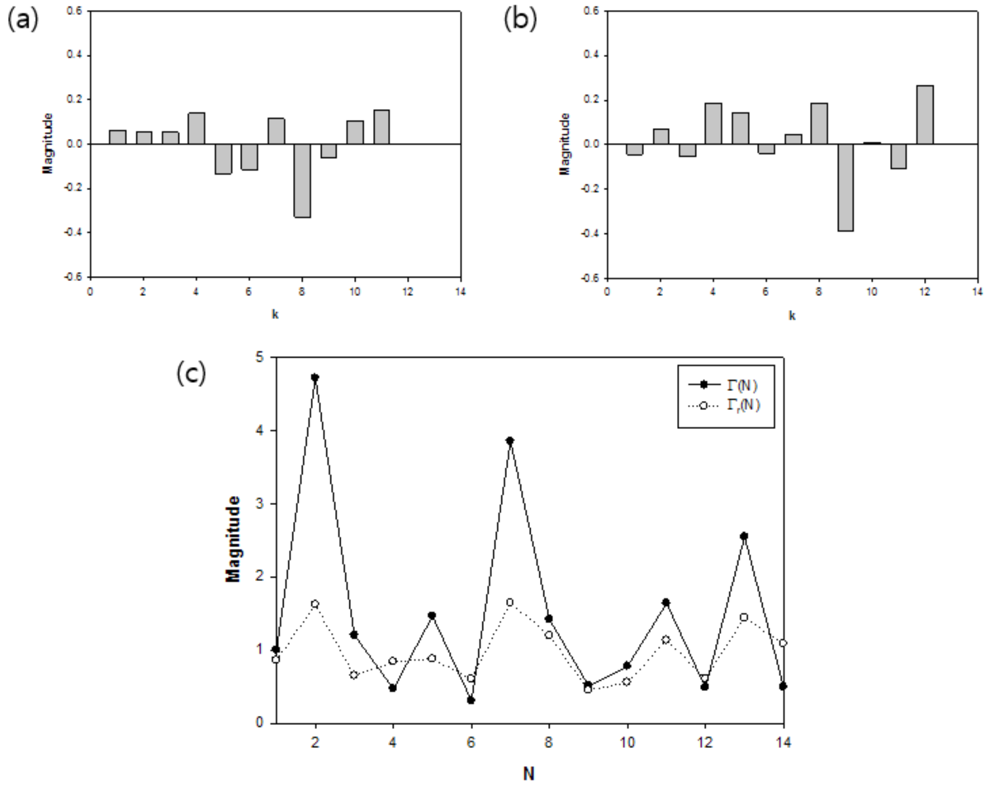

Fig. 5. Result DFA of $\Gamma(N)$ and rebuilt $\Gamma_r(N)$: (a) a_k, (b) b_k, and (c) $\Gamma(N)$.

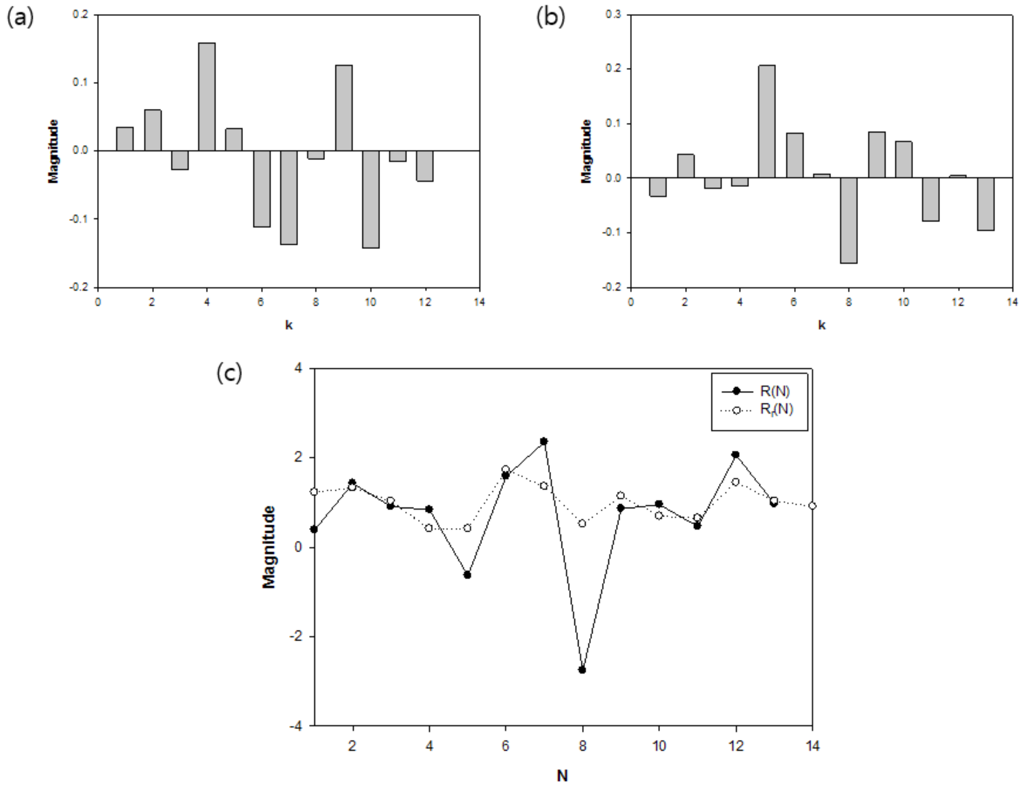

Fig. 6. Result DFA of $R(N)$ and rebuilt $R_r(N)$: (a) a_k, (b) b_k, and (c) $R(N)$.

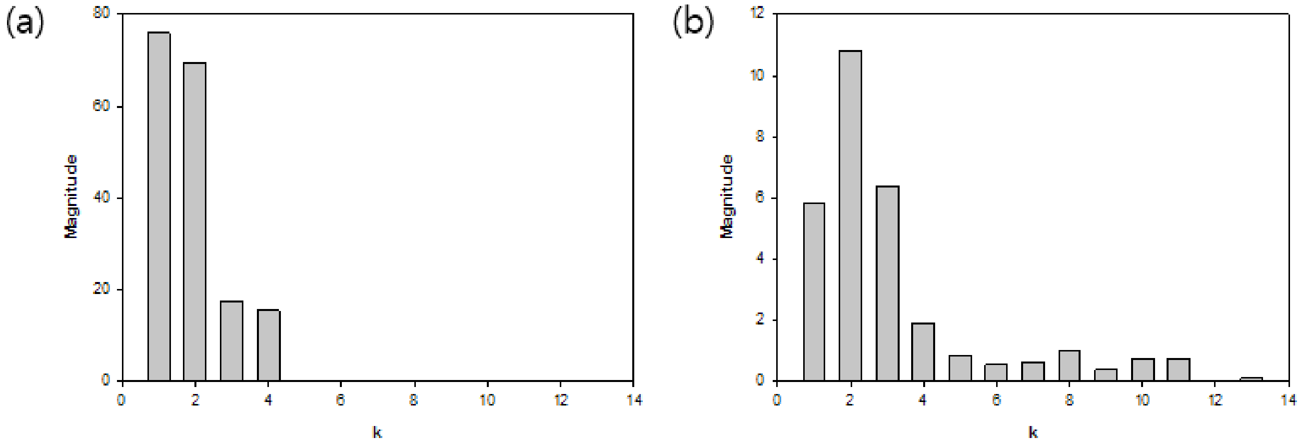

Fig. 7. Result DFA of NTU(N) and Flux(N): (a) d_k of NTU(N) and (b) d_k of Flux(N).

The slope $\alpha(N)$ needed to consider the trend of NTU, which was the degree of micro-particles in feed water because NTU were related with TMP slope at the same time. Micro-particles in feed water theoretically influenced the increase of TMP slope. When NTU(N) was put into the DFA, its frequency 'k' was 1, 2, 3, and 4 in Fig. 7(a), in which the number of results was small when comparing with other results because recorded NTU data were not enough in the period. And, $\alpha(N)$ also needed to consider the flux trend because its flux was related with TMP slope in the same time as given in Eqs. (3), (4), and (5). When Flux(N) was put into the DFA, its valid frequencies were 1, 2, 3, and 4 in Fig. 7(b), which showed the same results of NTU(N).

Some data in (N, $\alpha(N)$), such as (1, –0.7966), (7, –0.014), and (8, –0.0256) seems not to be proper values from the data analysis of TMP slope, because other $\alpha(N)$ values were positive as well as $\alpha(N)$ was theoretically positive under conventional operating circumstances. Except for these improper values, the average of the others was 0.2354 and its standard deviation was 0.1701, which showed that $\alpha(N)$ ranged from 0.0654 to 0.4055 with its confidence level, 68%. It could be assumed that $\alpha(N)$ was approximately positioned the interval between 0.06 and 0.5 with its confidence level, 70%. Based on the interval, $\alpha(N)$'s raw data were edited into 0.06 or 0.5 when $\alpha(N)$ was less than 0.6 or over 1.3, respectively.

These edited pieces of $\alpha(N)$ data were put into the DFA, which showed magnitudes of frequency as in Fig. 8(a) and (b). Thus, $\alpha(N)$ was rebuilt in Fig. 8(c) by these frequencies that were 1, 2, 3, and 4 in both 'a_k' and 'b_k' relating the DFA results of both NTU(N) and Flux(N). Residual frequencies were used to formulate the different trend of $\alpha(N)$ to find the deteriorated term 'α_d'. The slope of its linear regression was 0.0032 and positive value, which was considered as 'α_d' value, because $\alpha(N)$ would be increased slowly by membrane's deteriorations through micro-particles stacked on membranes' pores depending on Nth.

Rebuilt $\alpha_r(N)$'s mathematical formula is as shown in Eq. (24). Meanwhile, rebuilt $\alpha_r(0)$ was not zero but 0.1120, which could become membrane's characteristics.

$$\begin{aligned}\alpha_r(N) &= 0.0032\cdot N + 0.2094\\ &+ 0.0395\cdot\cos\left(\frac{\pi}{12}N-\frac{2\pi}{12}\right) - 0.0479\cdot\cos\left(\frac{2\pi}{12}N-\frac{2\pi}{12}\right)\\ &- 0.0265\cdot\cos\left(\frac{3\pi}{12}N-\frac{2\pi}{12}\right) - 0.0737\cdot\cos\left(\frac{4\pi}{12}N-\frac{2\pi}{12}\right)\\ &+ 0.0215\cdot\sin\left(\frac{3\pi}{12}N-\frac{2\pi}{12}\right) - 0.0723\cdot\sin\left(\frac{4\pi}{12}N-\frac{2\pi}{12}\right)\end{aligned} \tag{24}$$

4.3. Results of TMP simulation

This simulation results could be used to expect the values of TMP in the future as shown in Fig. 9 until N = 30. After 3,000 d, the simulation shows highly fluctuating. Main reasons came from the limit of the DFA as shown in Fig. 9(a). DFA has defects overflowing on its edge parts such as drastic fluctuations [65]. Hence, edge parts could not be used in the simulation results. Proper expected time will become about 3,000 d (N = 26). At the time, the CIP efficiency index, $E(N)$, becomes below 0.7 as shown in Fig. 9(b), in which the membrane modules could be determined as being exchanged to new ones.

The points in the time, when $E(N)$ was less than 0.7, were 24, 25, 26, and 30 in N domain. It has drastic changes from 26 to 30 in N, which was considered as the improper results including the DFA limit. The DFA analysis had overshooting occurrences in its edges, magnifying its uncertainty [66]. Therefore, these simulations result could estimate that its life span was 2,703 d, about 7.4 years (from N = 1 to N = 23) because $E(N)$ will become less than 0.7 at N = 23. Its residual usage time would technically become about 3.4 year from 1,472 d (N = 14).

4.4. Calculating its total O&M cost on N, and benefit–cost on N

$J_{\mathrm{TMP}}(N)$ is evaluated by dividing the electrical cost and operating cost coefficient by the area of TMP on Nth stage, respectively. The area of TMP is related to the electric cost on Nth stage. Based on the electrical cost from N = 1 to N = 14 in

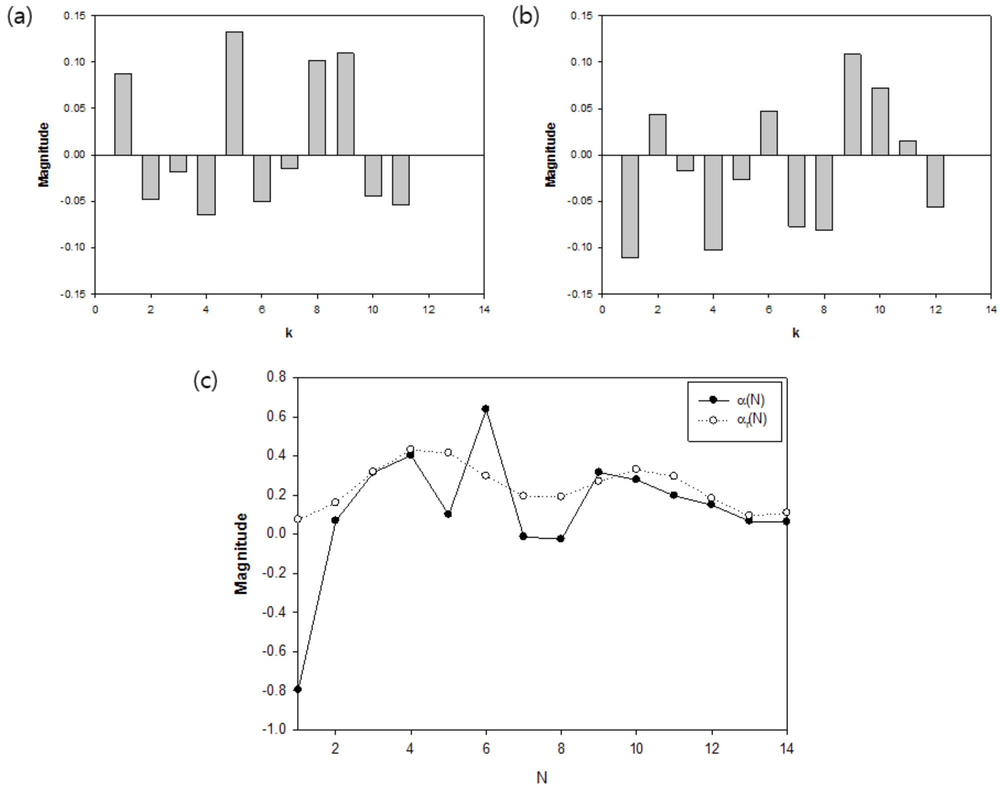

Fig. 8. Result DFA of $\alpha(N)$ and rebuilt $\alpha_r(N)$: (a) for a_k, (b) for b_k, and (c) for $\alpha(N)$.

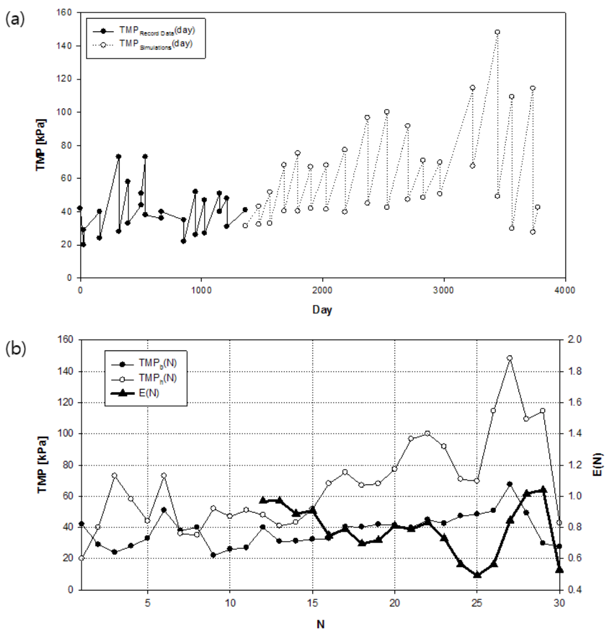

Fig. 9. Results of TMP simulation: (a) for TMP(day), (b) for $\text{TMP}_b(N)$, $\text{TMP}_h(N)$, and $E(N)$.

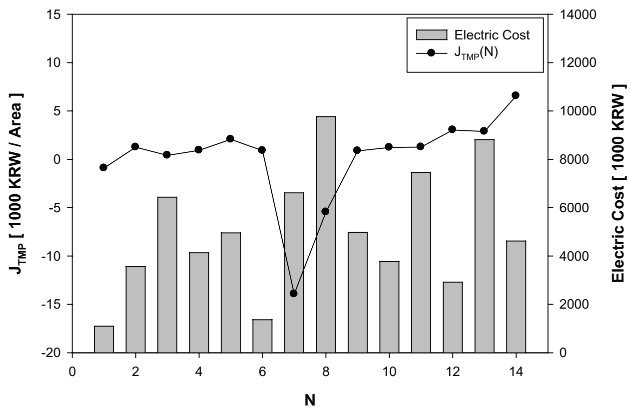

Fig. 10. Results of $J_{TMP}(N)$ and electrical cost(N) depending on Nth.

the plant, $J_{TMP}(N)$ is shown in Fig. 10. J_{TMP} was defined as the average of $J_{TMP}(N)$ values from $N = 1$ to $N = 14$ after removing its negative values where N was 1, 7, and 8 because J_{TMP} had to have positive values in the cost view as well as excepting for $J_{TMP}(14)$, 6.54, which unusually showed the biggest value comparing with proper ones. Thus, J_{TMP} was evaluated as USD 1.5/Area_{TMP}, which could be used to calculate the operational cost on Nth stage in TMP simulation. And operating cost on Nth stage, $C_{\text{Operation}}(N)$, could be estimated by using Eq. (25). Here, USD is the monetary unit of the United States of America, and KRW is the monetary unit of the Republic of Korea, and '1,000 KRW' was assumed to be approximately equal to '1 USD' in this study.

$$C_{\text{Operation}}\left(N\right) = J_{\text{TMP}} \cdot \text{Area}_{\text{TMP}}\left(N\right) \approx 1.5 \cdot \text{Area}_{\text{TMP}}\left(N\right) \tag{25}$$

Historical data of the direct O&M cost in 2014 are shown in Fig. 11. The sectional average cost per month in 2014 was individually calculated as follows: (a) feed water cost was estimated to be 2,883 USD/month, (b) chemical cost for CIP was estimated to be 261 USD/month, (c) operating electrical cost was estimated to be 1,761 USD/month, and (d) total labour cost was estimated to be 3,217 USD/month. Thus, the direct O&M cost per month was estimated to be USD 8,122, which is about 4.6 times of electrical cost per month. The direct O&M cost on Nth was calculated in Eq. (26), depending on the area of TMP on Nth.

$$C_{\text{DirectO\&M}}\left(N\right) \approx 4.6 \cdot C_{\text{Operation}}\left(N\right) \approx 6.9 \cdot \text{Area}_{\text{TMP}}\left(N\right) \tag{26}$$

This study supposed that the system's non-operating probability and module's failure probability as 2.34% per month for 100 months, equivalent to about 8.2 years by Poisson's failure model [67–69]. And the module's price is fixed to be USD 500. Thus, the indirect O&M cost depending on operating time on Nth, $\Delta t(N)$, was calculated by Eq. (27). It shows that its indirect O&M cost would be marginal to its direct O&M cost on Nth stage.

$$C_{\text{Indirect}}\left(N\right) \approx 23.2 \cdot \Delta t\left(N\right) \tag{27}$$

Therefore, total O&M cost on Nth stage, $C_{\text{TotalO\&M}}$, is shown in Eq. (28), combining the direct and the indirect one.

$$C_{\text{TotalO\&M}}\left(N\right) \approx 6.9 \cdot \text{Area}_{\text{TMP}}\left(N\right) + 23.2 \cdot \Delta t\left(N\right) \tag{28}$$

Also, the benefit coefficient on Nth, J_{Water} was roughly considered as 0.100 USD/ton because the plant had been operated with its direct benefit under its practical cost in produced water, which is approximately ranged from 0.080 to 0.090 USD/ton for that period. Furthermore, its average of produced water quantity on a day from $N = 1$ to $N = 13$ was 3,908.58 m^3/d (≃ton/d), which was used as $Q(N)$ value in the further simulating period. Thus, the benefit–cost on Nth stage, $B_{\text{Produce}}(N)$, was simply evaluated in Eq. (29) without including the indirect benefit–cost.

$$B_{\text{Produce}}\left(N\right) \approx 390.9 \cdot \Delta t\left(N\right) \tag{29}$$

4.5. Results of B/C analysis and discussion

Benefit per cost ratio (B/C) showed the economical usefulness in the aspect of O&M for the plant. When B/C was less than one, it means that the plant was not profitable during its operation. Thus, the plant needs to reduce its O&M costs, or increase its benefit coefficient to make better benefit. The net profit (S) was defined by balancing its benefit–cost and O&M cost, which showed if the amount of its renewal costs could be made, or not.

In the plant, the results of both $B/C(N)$ and $E(N)$ on Nth stage are shown in Fig. 12. And the results of both $B/C(N)$ and $S(N)$ are also shown in Fig. 13. $B/C(N)$ was dropped as much as N had increased, which meant losing its economic efficiency within $N = 17$. Furthermore, when N had increased from 17 to 23, $S(N)$ had drastically enlarged negative values,

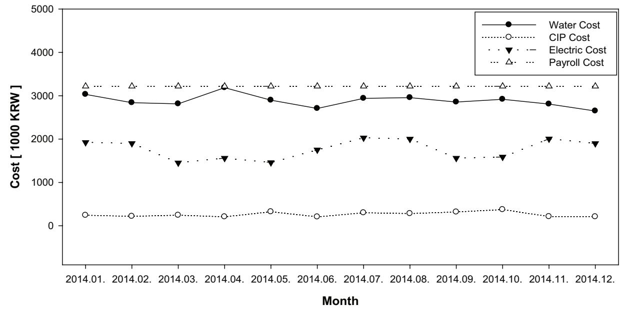

Fig. 11. Recorded data of operation and direct maintenance costs in 2014.

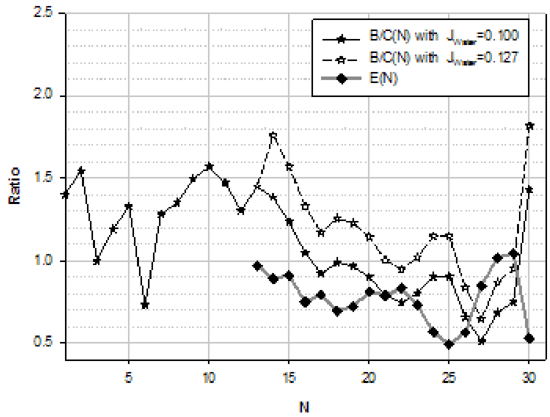

Fig. 12. Simulation results of $B/C(N)$ and $E(N)$.

showing that its economic feasibility was lost (Fig. 13(a)). Thus, its economic life span could become $N = 17$ when it was within about 1 year from $N = 14$, which was much earlier than its technical life spot ($N = 23$). Its technical life span showed that the plant could be used without severe operating problems by $N = 23$. Thus, the plant reasonably needs to extend its economic life spot by its technical life span through increasing its benefit coefficient (J_{Water}), or decreasing O&M cost after $N = 14$.

In order to extend its economic life span by its technical one, the scenario increasing its benefit coefficient was strategically preferable for O&M. The increasing amount of J_{Water} could become at least 0.027 USD/ton based on the outcome of the simulation, resulting in which the plant would be possible to extend its economic life span from $N = 14$ to $N = 23$ (having more than 3.37 years), as well as making its replacing cost of PHFM modules by the sum of $S(N)$ from $N = 14$ to $N = 23$,which is shown in Fig. 13(b). It meant that the plant could more strategically prepare its O&M plan by using the method in the future, which is expected to increase its O&M efficiency in the long-term for 3 years.

5. Conclusion

The life span of PHFM modules and O&M efficiency could be evaluated by an AM method such as TMP simulation and B/C analysis. Simulation results showed that replacements of membrane modules were anticipated to be

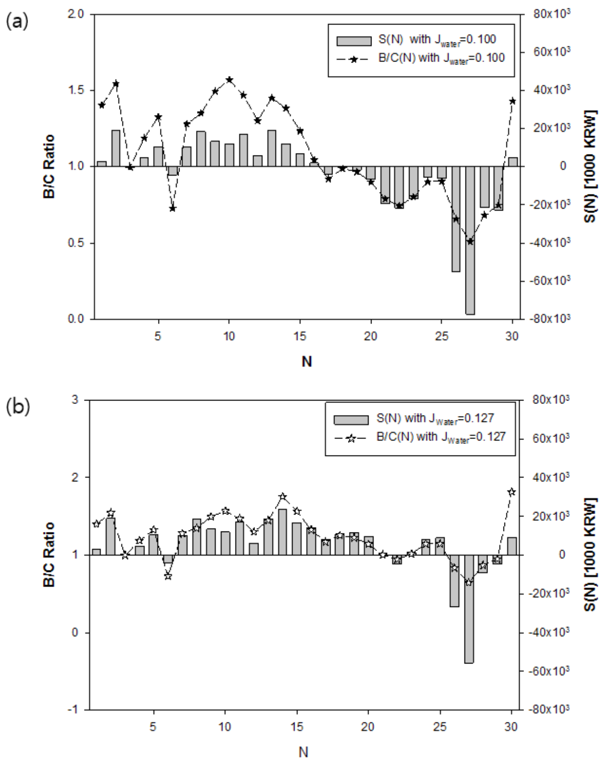

Fig. 13. Simulation results of $B/C(N)$ and $S(N)$: (a) for J_{Water} = 0.100 and (b) for J_{Water} = 0.127.

March 2018 for technical efficiency, or September 2015 for economic efficiency if J_{Water} was constantly 0.100. However, the economic life span could be improved by March 2018 when J_{Water} was raised to 0.127 from N = 14 to N = 23. And then, facility will secure the longevity without financial burdens through the minimum raise, 0.027 USD/ton in the water price. TMP trend would steadily increase in a few years, inducing diverse potential technical problems frequently in the system as well as loading on its financial. Thus, the plant will need to prepare the replacement plan of PHFM modules and improve the O&M efficiency in near future. From this study, the analyzed model based on an AM concept could draw the life span of membrane modules and help making better O&M plans for a water treatment plant.

Acknowledgement

This study has been supported by the Korean Ministry of Environment as 'Projects for Public Welfare Technology Development (2014000700003)'.

References

[1] C. Gimenez, V. Sierra, J. Rodon, Sustainable operations: their impact on the triple bottom line, Int. J. Prod. Econ., 140 (2012) 149–159.

[2] M. Shahidehpour, R. Ferrero, Time management for assets: chronological strategies for power system asset management, IEEE Power Energy Mag., 3 (2005) 32–38.

[3] H. Alegre, M. do Céu Almeida, Strategic Asset Management of Water Supply and Wastewater Infrastructures, IWA Publishing, London, UK, 2009, pp. 26–41.

[4] D.J. Vanier, Asset management: "A" to "Z", NRCC/CPWA/IPWEA Seminar Series "Innovations in Urban Infrastructure", Philadelphia, USA, 2001.

[5] E. Richard. Brown, J.H. Spare, Asset Management, Risk, and Distribution System Planning, Power Systems Conference and Exposition IEEE PES, New York, USA, 2004.

[6] R.E. Brown, E. Richard, Aging Distribution Infrastructure at Pacific Gas and Electric, Pacific and Electric Company, San Francisco, 2005.

[7] H. Kim, J.G. Im, S.R. An, It is time to take an interest in asset management of infrastructure, J. Korean Soc. Civil Eng., 62 (2014) 10–19.

[8] S. Park, S.I. Park, S.H. Lee, Strategy on sustainable infrastructure asset management: focus on Korea's future policy directivity, Renew. Sustain. Energy Rev., 62 (2016) 710–722.

[9] J.S. Taylor, L. Mulford, S.J. Duranceau, Cost and performance of a membrane pilot plant, J. Am. Water Resour. Assoc., 81 (1989) 52–60.

[10] T. Asano et al., Water reuse: issues, technologies, and applications, McGraw Hill, New York, USA, 2006.

[11] G. Owen, M. Bandi, J.A. Howell, S.J. Churchouse, Economic assessment of membrane processes for water and waste water treatment, J. Membr. Sci., 102 (1995) 77–91.

[12] B. Van der Bruggen, M. Mänttäri, M. Nyström, Drawbacks of applying nanofiltration and how to avoid them: a review, Sep. Purif. Technol., 63 (2008) 251–263.

[13] Z. Wang, J. Ma, C.Y. Tang, K. Kimura, Q. Wang, Membrane cleaning in membrane bioreactors: a review, J. Membr. Sci., 468 (2014) 276–307.

[14] Z. Wang, Z. Wu, X. Yin, L. Tian, Membrane fouling in a submerged membrane bioreactor (MBR) under sub-critical flux operation: membrane foulant and gel layer characterization, J. Membr. Sci., 325 (2008) 238–244.

[15] D. Kuzmenko, E. Arkhangelsky, S. Belfer, V. Freger, V. Gitis, Chemical cleaning of UF membranes fouled by BSA, Desalination, 179 (2005) 323–333.

[16] S.J. Judd, P. Hillis, Optimisation of combined coagulation and microfiltration for water treatment, Water Res., 35 (2001) 2895–2904.

[17] S. Yao, M. Costello, A.G. Fane, J.M. Pope, Non-invasive observation of flow profiles and polarisation layers in hollow fibre membrane filtration modules using NMR micro-imaging, J. Membr. Sci., 99 (1995) 207–216.

[18] L. Martinelli, C. Guigui, A. Line, Characterisation of hydrodynamics induced by air injection related to membrane fouling behaviour, Desalination, 250 (2010) 587–591.

[19] A. Hernández, J.I. Calvo, P. Prádanos., F. Tejerina, Pore size distributions in micro-porous membranes: a critical analysis of the bubble point extended method, J. Membr. Sci., 112 (1996) 1–12.

[20] A. Mey-Marom, M.G. Katz, Measurement of active pore size distribution of microporous membranes-a new approach, J. Membr. Sci., 27 (1986) 119–130.

[21] B.D. Cho, A.G. Fane, Fouling transients in nominally subcritical flux operation of a membrane bioreactor, J. Membr. Sci., 209 (2002) 391–403.

[22] P.J. Smith, S. Vigneswaran, H.H. Ngo, R. Ben-Aim, H. Nguyen, A new approach to backwash initiation in membrane systems, J. Membr. Sci., 278 (2006) 381–389.

[23] D.J.D. Vanier, Why industry needs asset management tools, J. Comput. Civil Eng., 15 (2001) 35–43.

[24] J.C.M. Lucio, J.L.T. Nunes, R.C.G. Teive, Asset Management into Practice: A Case Study of a Brazilian Electrical Energy Utility, Intelligent System Applications to Power Systems, ISAP'09, 15th International Conference IEEE, 2009.

[25] S. Singh, K.C. Khulbe, T. Matsuura, P. Ramamurthy, Membrane characterization by solute transport and atomic force microscopy, J. Membr. Sci., 142 (1998) 111–127.

[26] S.I. Nakao, S. Kimura, Models of membrane transport phenomena and their applications for ultrafiltration data, J. Chem. Eng. Jpn., 15 (1982) 200–205.

[27] S. Chang, A.G. Fane, T.D. Waite, Analysis of constant permeate flow filtration using dead-end hollow fiber membranes, J. Membr. Sci., 268 (2006) 132–141.

[28] G. Belfort, R.H. Davis, A.L. Zydney, The behaviour of suspensions and macromolecular solutions in cross flow microfiltration, J. Membr. Sci., 96 (1994) 1–58.
[29] J.H. Tay, P. Yang, W.Q. Zhuang, S.T.L. Tay, Z.H. Pan, Reactor performance and membrane filtration in aerobic granular sludge membrane bioreactor, J. Membr. Sci., 304 (2007) 24–32.
[30] S. Khirani, P.J. Smith, M.H. Manéro, R.B. Aim, S. Vigneswaran, Effect of periodic backwash in the submerged membrane adsorption hybrid system (SMAHS) for wastewater treatment, Desalination, 191 (2006) 27–34.
[31] R.W. Field, D. Wu, J.A. Howell, B.B. Gupta, Critical flux concept for microfiltration fouling, J. Membr. Sci., 100 (1995) 259–272.
[32] R. Rosberg, Ultrafiltration (new technology), a viable cost-saving pretreatment for reverse osmosis and nanofiltration: a new approach to reduce costs, Desalination, 110 (1997) 107–113.
[33] J. Radjenović, M. Matošić, I. Mijatović, M. Petrović, D. Barceló, Membrane Bioreactor (MBR) as an Advanced Wastewater Treatment Technology, Emerging Contaminants from Industrial and Municipal Waste, Springer, Berlin, Heidelberg, 2008, pp. 37–101.
[34] E. Arkhangelsky, D. Kuzmenko, V. Gitis, Impact of chemical cleaning on properties and functioning of polyethersulfone membranes, J. Membr. Sci., 305 (2007) 176–184.
[35] A. Simon, W.E. Price, L.D. Nghiem, Changes in surface properties and separation efficiency of a nanofiltration membrane after repeated fouling and chemical cleaning cycles, Sep. Purif. Technol., 113 (2013) 42–50.
[36] A. Al-Amoudi, P. Williams, A.S. Al-Hobaib, R.W. Lovitt, Cleaning results of new and fouled nanofiltration membrane characterized by contact angle, updated DSPM, flux and salts rejection, Appl. Surf. Sci., 254 (2008) 3983–3992.
[37] A. Al-Amoudi, P. Williams, S. Mandale, R.W. Lovitt, Cleaning results of new and fouled nanofiltration membrane characterized by zeta potential and permeability, Sep. Purif. Technol., 54 (2007) 234–240.
[38] A. Simon, W.E. Price, L.D. Nghiem, Effects of chemical cleaning on the nanofiltration of pharmaceutically active compounds (PhACs), Sep. Purif. Technol., 88 (2012) 208–215.
[39] R. Liikanen, J. Yli-Kuivila, R. Laukkanen, Efficiency of various chemical cleanings for nanofiltration membrane fouled by conventionally-treated surface water, J. Membr. Sci., 195 (2002) 265–276.
[40] K. Košutić, B. Kunst, RO and NF membrane fouling and cleaning and pore size distribution variations, Desalination, 150 (2002) 113–120.
[41] N. Ueda, Optimal linear combination of neural networks for improving classification performance, IEEE Trans. Pattern Anal. Mach. Intell., 22 (2000) 207–215.
[42] C. Regula, E. Carretier, Y. Wyart, G. Gésan-Guiziou, A. Vincent, D. Boudot, P. Moulin, Chemical cleaning/disinfection and ageing of organic UF membranes: a review, Water Res., 56 (2014) 325–365.
[43] R. Suthanthararajan, E. Ravindranath, K. Chits, B. Umamaheswari, T. Ramesh, S. Rajamam, Membrane application for recovery and reuse of water from treated tannery wastewater, Desalination, 164 (2004) 151–156.
[44] R.E. Brown, Failure Rate Modelling Using Equipment Inspection Data, Power Engineering Society General Meeting IEEE, 2004.
[45] A.F. Viero, G.L. Sant'Anna, R. Nobrega, The use of polyetherimide hollow fibres in a submerged membrane bioreactor operating with air backwashing, J. Membr. Sci., 302 (2007) 127–135.
[46] S. Robinson, S.Z. Abdullah, P. Bérubé, P. Bérubé, P. Le-Clech, Ageing of membranes for water treatment: linking changes to performance, J. Membr. Sci., 503 (2016) 177–187.
[47] R. Cutler, L. Davis, View-Based Detection and Analysis of Periodic Motion, Pattern Recognition, Proc. Fourteenth International Conference, Vol. 1, IEEE, 1998.
[48] R.G. White, J.G. Walker, Noise and Vibration, Ellis Horwood Ltd, Herts UK, 1982.
[49] M.L. Boas, Mathematical Methods in the Physical Sciences, DePaul University, Chicago, 2006, pp. 361–372.
[50] A.V. Oppenheim, Discrete-Time Signal Processing, Prentice-Hall, Upper Saddle River, NJ, 1999, pp. 98–130.
[51] S. Weinstein, P. Ebert, Data transmission by frequency-division multiplexing using the discrete Fourier transform, IEEE Trans. Commun. Technol., 19 (1971) 628–634.
[52] J. Drèze, N. Stern, The Theory of Cost-Benefit Analysis, Handbook of Public Economics, Vol. 2, 1987, pp. 909–989.
[53] H.N. Jo, J.K. Lim, Y.M. Choe, K.H. Paek, Life-Cycle Cost Analysis for Infrastructure Systems, Goomi Book, Seoul, 2009.
[54] P. Jorion, Risk 2: Measuring the risk in value at risk, Finance Anal. J., 52 (1996) 47–56.
[55] R.T. Rockafellar, S. Uryasev, Optimization of conditional value-at-risk, J. Risk, 2 (2000) 21–42.
[56] D.E. Nordgard, G. Solum, Experiences Using Quantitative Risk Assessment in Distribution System Asset Management, Electricity Distribution-Part 1 CIRED, 2009, p. 171.
[57] M.M. Hufschmidt, Benefit-cost analysis, J. Contemp. Water Res. Educ., 116 (2011) 11.
[58] S. Hajkowicz, R. Spencer, A. Higgins, O. Marinoni, Evaluating water quality investments using cost utility analysis, J. Environ. Manage., 88 (2008) 1601–1610.
[59] M.R. Haghifam, E. Akhavan-Rezai, A. Fereidunian, An Asset Management Approach to Momentary Failure Risk Analysis on MV Overhead Lines, Probabilistic Methods Applied to Power Systems (PMAPS), IEEE 11th International Conference, 2010.
[60] R. Robinson, Economic evaluation and health care, BMJ, 307 (1993) 726.
[61] A. Schneider, G. Hommel, M. Blettner, Linear regression analysis: part 14 of a series on evaluation of scientific publications, Dtsch Arztebl Int., 107 (2010) 776–822.
[62] K.J. Kim, H. Moskowitz, M. Koksalan, Fuzzy versus statistical linear regression, Eur. J. Oper. Res., 92 (1996) 417–434.
[63] S.R. Lipsitz, T. Leong, J. Ibrahim, S. Lipshultz, A partial correlation coefficient and coefficient of determination for multivariate normal repeated measures data, Statistician, (2001) 87–95.
[64] H. Holttinen, M. Milligan, B. Kirby, T. Acker, V. Neimane, T. Molinshi, Using standard deviation as a measure of increased operational reserve requirement for wind power, Wind Eng., 32 (2008) 355–377.
[65] L. Li, Use of Fourier series in the analysis of discontinuous periodic structures, J. Opt. Soc. Am. A, 13 (1996) 1870–1876.
[66] W.F. Schreiber, D.E. Troxel, Transformation between continuous and discrete representations of images: a perceptual approach, IEEE Trans. Pattern Anal. Mach. Intell., 2 (1985) 178–186.
[67] C.S. Lee, Y.W. Nam, D.I. Kim, Economical selection of optimum pressurized hollow fiber membrane modules in water purification system using RbLCC, J. Membr. Water Treat., 8 (2017) 137–147.
[68] W.H. Tang, A. Ang, Probability Concepts in Engineering: Emphasis on Applications to Civil & Environmental Engineering, Wiley, 2007, pp.145–146.
[69] F. Li, R.E. Brown, A cost-effective approach of prioritizing distribution maintenance based on system reliability, IEEE Trans. Power Delivery, 19 (2004) 439–441.